

J. Frauhammer¹ H. Klein² G. Eigenberger¹ U. Nowak

Solving moving boundary problems with an
adaptive moving grid method:
Rotary heat exchangers
with condensation and evaporation

¹ Universität Stuttgart, Institut für Chemische Verfahrenstechnik,
Böblinger Straße 72, 70199 Stuttgart, Germany.

² Linde AG, Werksgruppe Verfahrenstechnik und Anlagenbau
Dr. Carl-von-Linde-Straße 6-14, 82049 Höllriegelskreuth, Germany

Solving moving boundary problems with an adaptive moving grid method: Rotary heat exchangers with condensation and evaporation

Jörg Frauhammer[†], Harald Klein[‡], Gerhart Eigenberger[†] and Ulrich Nowak[§]

[†]Universität Stuttgart, Institut für Chemische Verfahrenstechnik,
Böblinger Straße 72, 70199 Stuttgart, Germany.

[‡] Linde AG, Werksgruppe Verfahrenstechnik und Anlagenbau
Dr. Carl-von-Linde-Straße 6-14, 82049 Höllriegelskreuth, Germany

[§] Konrad-Zuse-Zentrum für Informationstechnik,
Takusstraße 7, 14195 Berlin-Dahlem, Germany

1 Abstract

A numerical method for the treatment of moving discontinuities in the model equations of chemical engineering systems is presented. The derived model describing the effects of condensation and evaporation in a regenerative air to air heat exchanger yields an illustrative example for these so called moving boundary problems. The presented adaptive moving grid method is based on the algorithm PDEX for parabolic partial differential equations. It is shown that the method is suited for problems where the arising discontinuities cause low rates of convergence if the equations are solved with a static grid.

2 Introduction

The handling of spatial discontinuities in models of chemical engineering systems is straightforward if their location is fixed. An example is a fixed bed reactor with different thermodynamic or structural properties of the solid bed like inert and catalytic regions where the governing equations vary from one part of the reactor to another. The problem of spatial discontinuities becomes more difficult to handle if the point where the model equations have to be switched moves along with the simulation time. These problems are called moving boundary problems and arise in many areas of chemical engineering. Well known examples are gas-solid reactions in a pellet [4] and the homogeneous or heterogeneous chemical reaction with zero order reaction rate for one of the reactants [1].

For zero order reactions the spatial domain is separated into a region with educt concentration greater than zero where the reaction rate is constant and an adjacent region with educt concentration equal zero, where the rate is zero. During dynamic simulation, the boundary between the two regions moves with time along the space coordinate and represents a moving boundary which is characterised by a discontinuity in the governing model equations.

Another illustrative example of a moving boundary problem presented in this paper is a regenerative air to air heat exchanger widely used in air conditioning systems [22, 37, 38, 39, 40]. A warm air stream heats up a cold metal matrix during the first period, in the second period a cold air stream flows through the warm matrix while absorbing heat from the solid storage material. In order to obtain a pseudo-continuous operation either a multi-bed design with periodic feed switches or a rotary type of heat exchanger is used [23, 26, 41]. If the air stream is moist, water vapor will condense if the temperature of the matrix is below the dew point temperature of the air. In this period the matrix is wetted with a thin film of liquid water. During the next period the water may evaporate into the dry air stream. On the matrix dry and wet parts may exist next to each other. Depending on whether the matrix is wet water can evaporate into the air passing the surface such that the dry and the wet parts of the matrix must be described by a different set of model equations. The boundaries separating these regions are moving during the process and must be recognized during the simulation. This example has been selected to illustrate the problems which arise and to show how they can be handled. The method presented can be applied to solve other spatially 1D moving boundary problems as well.

Moving grid methods have been proposed recently to solve 1D problems where steep wave fronts arise [5, 31, 33, 42]. The grid points move during one time step along with the propagating front. One aim is to make a static grid adaption unnecessary and to reduce the dynamics of the system on the other hand such that the change of the state variables are minimized which results in larger time steps during the simulation. For an overview about moving grid methods we refer to Furzeland et al. [17]. In this paper it will be shown that problems with moving boundaries and moving

discontinuities can be solved very efficiently using such a moving grid method. The algorithm presented is a modification of the one developed by Nowak [27]. Using the example of a regenerative air to air heat exchanger with non-hygroscopic material a new method to follow points with discontinuities will be developed and tested.

3 Modelling of heat and mass transfer by condensation and evaporation

Heat transfer with condensation of water vapor out of noncondensable gases such as air onto a solid surface has been treated in a large number of theoretical and experimental publications. A major topic in many papers is the description of fog formation followed by condensation in a thermal boundary layer next to a cold surface [15, 25, 34]. If condensation occurs, the rate of heat and mass transfer usually changes over a wide range. Therefore, the aim is to describe the effect of condensation in the boundary layer to determine the different heat and mass transfer in general [6, 7, 8, 9, 10, 21, 24].

A common way to describe the heat and mass transfer from a noncondensable gas on a solid surface is a 2D-formulation with the radial coordinate r perpendicular to the axial flow direction z . For small concentrations of water vapor *Fick's law of Diffusion* can be applied:

$$\dot{n}_W = -D \cdot \frac{\partial c_W}{\partial r} \quad (1)$$

Herein c_W denotes the molar concentration of water in the boundary layer. For higher concentrations the so called *Stefan-Flow* [6] is appropriate which takes into account that the noncondensable gas does neither adsorb nor desorb at the wall (c denotes the total molar concentration of the gas):

$$\dot{n}_W = -D \cdot \frac{c}{c - c_W} \cdot \frac{\partial c_W}{\partial r} \quad (2)$$

The boundary condition at the wall is

$$c_W = c_M \quad (3)$$

where c_M is the equilibrium concentration of the condensate film which only depends on its temperature. Analytical solutions of Eqn. (1) or (2) have been adapted for special cases. In a 1D-description the linear driving force estimation can be used:

$$\dot{n}_W = \beta \cdot (c_W - c_M) \quad (4)$$

A review of the literature indicated that the methods described above are mostly used to describe the condensation out of a noncondensable gas onto a solid surface.

For conditions where evaporation from a wet solid surface occurs, Eqn. (1), (2) or (4) can be still applied. One difference is the direction of the driving gradient and therefore the direction of the vapor flux. Whereas condensation can occur no matter whether the solid surface is wet or dry, evaporation requires a driving gradient from the surface to the gas stream **and** a liquid water film on the surface. Therefore, it is very important to know the boundaries between wet and dry parts, especially if they change during transient operation in regenerative heat exchangers [39].

This problem was first recognized by Hausen [20] who splitted the cold period into a wet and a dry part. Whereas Hausen's work emphasized cold temperature applications, the investigations of van Leersum [37] and Vauth [40] describe condensation and evaporation in air to air regenerators using the linear driving force estimation in Eqn. (4) which will be used in this paper, too. Certain effects like condensation and fog formation in the boundary layer are not taken into account.

Fig. 1 shows one flow channel of a regenerative heat exchanger. The condition for condensation at a specific point z in the flow channel is that the actual vapor pressure of water in the air stream is higher than the saturation vapor pressure over the liquid water film, *i.e.* $p_W(t, z) > p_W^{sat}$. Evaporation of liquid water from the solid surface can occur only if the matrix is wet. At a specific point z water evaporates from a wet surface into the moist air if the saturation vapor pressure is higher than the vapor pressure of water $p_W(t, z)$ in the air, *i.e.* $p_W^{sat} > p_W(t, z)$.

Instead of the partial vapor pressure of water p_W the water content in the air X_A will be used where X_A is defined as the fraction of mass of water vapor in the air m_W to the mass of dry air m_A :

$$X_A = \frac{m_W}{m_A} \quad (5)$$

and

$$X_A = \frac{M_W}{M_A} \cdot \frac{p_W}{p - p_W} = 0.622 \cdot \frac{p_W}{p - p_W} . \quad (6)$$

The regenerator surface consists of a macroporous layer which is thick enough to accumulate all of the condensed water vapor. Hence, no liquid movement will be considered and the water content Y_M of the matrix is defined by the mass of the liquid water m_M^W divided by the mass of the dry solid matrix m_S :

$$Y_M = \frac{m_M^W}{m_S} \quad (7)$$

The flow channel of a regenerative heat exchanger in Fig. 1 can be described by the heterogeneous model shown in Fig. 2. One phase consists of the flowing air, the second phase of the solid surface including the macroporous surface layer with the liquid water film (if present). The two phases are coupled through combined heat and mass transfer. The heat flux will be treated in detail in App. A.4. The driving force for the flux of water vapor from the moist air to the wetted matrix surface is

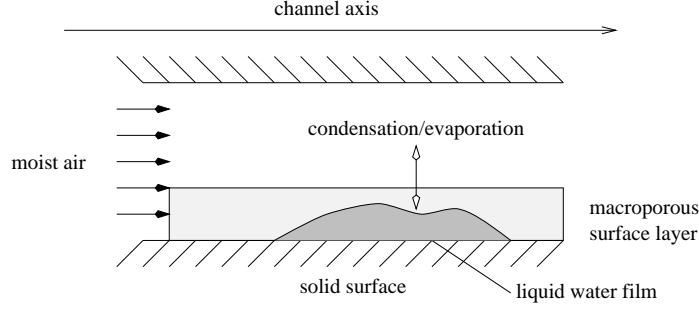


Figure 1: Condensation and evaporation in the flow channel of a regenerative heat exchanger

the difference between the the water content X_A of the air stream and the water content X_M of the air which is in equilibrium with the liquid water film:

$$d\dot{m}_W = \beta \cdot dA_s \cdot (X_A - X_M) \quad (8)$$

Since the water film is very thin it can be assumed that it will have the same temperature as the solid matrix [40], such that

$$X_M = X_M^{sat}(\vartheta_M) = 0.622 \cdot \frac{p_W^{sat}(\vartheta_M)}{p - p_W^{sat}(\vartheta_M)}. \quad (9)$$

The saturation vapor pressure p_W^{sat} has to be calculated as a function of the matrix temperature and the following correlation will be used [2]:

$$p_W^{sat} = \frac{c_1}{T_M} + c_2 + c_3 \cdot T_M + c_4 \cdot T_M^2 + c_5 \cdot T_M^4 + c_6 \cdot T_M^4 + c_7 \cdot \log(T_M) \quad (10)$$

with

$$T_M = \vartheta_M + 273.15$$

Condensation occurs if the water content of the moist air X_A is higher than the saturation value $X_M(\vartheta_M)$. Liquid water evaporates from the matrix if X_A is lower than $X_M(\vartheta_M)$ and the matrix is wet, *i.e.* $Y_M > 0$.

4 Balance equations and boundary conditions

The following system of equations has been derived in App. A for the control volume of Fig. 2. It describes the heat and mass transfer in the flow channel of a regenerative heat exchanger:

$$\varepsilon \cdot \varrho_A \cdot \frac{\partial X_A}{\partial t} = -\varepsilon \cdot \varrho_A \cdot v_A \cdot \frac{\partial X_A}{\partial z} + \varepsilon \cdot D_{eff} \cdot \frac{\partial^2 X_A}{\partial z^2} - \delta \cdot a_V \cdot \beta \cdot (X_A - X_M) \quad (11)$$

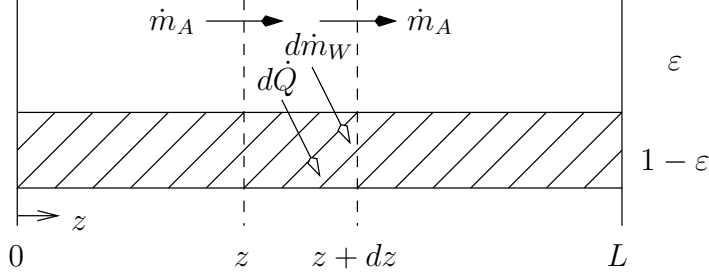


Figure 2: Heterogeneous model for condensation and evaporation in the flow channel of a regenerative heat exchanger

$$0 = X_M - 0.622 \cdot \frac{p_W^{sat}(\vartheta_M)}{p - p_W^{sat}(\vartheta_M)} \quad (12)$$

$$(1 - \varepsilon) \cdot \varrho_S \cdot \frac{\partial Y_M}{\partial t} = \delta \cdot a_V \cdot \beta \cdot (X_A - X_M) \quad (13)$$

$$\begin{aligned} \varepsilon \cdot \varrho_A \cdot c_p \cdot \frac{\partial \vartheta_A}{\partial t} &= -\varepsilon \cdot \varrho_A \cdot v_A \cdot c_p \cdot \frac{\partial \vartheta_A}{\partial z} \\ &+ \varepsilon \cdot D_{eff} \cdot c_{p,W} \cdot \frac{\partial X_A}{\partial z} \cdot \frac{\partial \vartheta_A}{\partial z} \\ &+ \varepsilon \cdot \lambda_{eff} \cdot \frac{\partial^2 \vartheta_A}{\partial z^2} - a_V \cdot \alpha \cdot (\vartheta_A - \vartheta_M) \end{aligned} \quad (14)$$

$$\begin{aligned} (1 - \varepsilon) \cdot \varrho_S \cdot c_M \cdot \frac{\partial \vartheta_M}{\partial t} &= (1 - \varepsilon) \cdot \lambda_S \cdot \frac{\partial^2 \vartheta_M}{\partial z^2} + a_V \cdot \alpha \cdot (\vartheta_A - \vartheta_M) \\ &+ \delta \cdot a_V \cdot \beta \cdot (X_A - X_M) \\ &\cdot (r_0 + c_{p,W} \cdot \vartheta_A - c_W \cdot \vartheta_M) \end{aligned} \quad (15)$$

$$\frac{\partial p}{\partial z} = -\frac{32 \cdot \nu \cdot \varrho_A \cdot v_A}{d_h^2} \quad (16)$$

The equations described in App. A do not apply for all cases arising in regenerative heat exchangers. The distinction is whether only condensation or both condensation and evaporation can occur (see Sect. 3). This distinction can be described in the system above using the step-function δ where

$$\delta = 1 \quad \text{if} \quad Y_M > 0, \quad (17)$$

$$\delta = 1 \quad \text{if} \quad Y_M = 0 \quad \text{and} \quad X_A \geq X_M, \quad (18)$$

$$\delta = 0 \quad \text{if} \quad Y_M = 0 \quad \text{and} \quad X_A < X_M. \quad (19)$$

The appropriate boundary conditions for the energy balance of the matrix are:

$$\left. \frac{\partial \vartheta_M}{\partial z} \right|_{z=0} = 0 \quad (20)$$

$$\left. \frac{\partial \vartheta_M}{\partial z} \right|_{z=L} = 0 \quad (21)$$

For the mass balance of the gas we find

$$D_{eff} \cdot \frac{\partial X_A}{\partial z} \Big|_{z=0} = \varrho_A \cdot v_A \cdot [X_A(z=0) - X_A^*] \quad (22)$$

$$\frac{\partial X_A}{\partial z} \Big|_{z=L} = 0. \quad (23)$$

The derivation of the boundary conditions for the energy balance of the gas yields

$$\lambda_{eff} \cdot \frac{\partial \vartheta_A}{\partial z} \Big|_{z=0} = \varrho_A \cdot v_A \cdot (c_{p,A} + X_A^* \cdot c_{p,W}) \cdot (\vartheta_A(z=0) - \vartheta_A^*) \quad (24)$$

$$\frac{\partial \vartheta_A}{\partial z} \Big|_{z=L} = 0. \quad (25)$$

The boundary condition for the pressure at the inlet is

$$p(z=0) = p^*. \quad (26)$$

In order to solve the system of Eqns. (11) - (16) initial conditions for the dynamic state variables are required ($0 \leq z \leq L$):

$$X_A(t=0, z) = X_A^0 \quad (27)$$

$$Y_M(t=0, z) = Y_M^0 \quad (28)$$

$$\vartheta_A(t=0, z) = \vartheta_A^0 \quad (29)$$

$$\vartheta_M(t=0, z) = \vartheta_M^0 \quad (30)$$

Formally, the system of model equations can be written as

$$\bar{B} \cdot \frac{\partial \vec{y}}{\partial t} = -\bar{v} \cdot \frac{\partial \vec{y}}{\partial z} + \frac{\partial}{\partial z} \cdot \left(\bar{D} \cdot \frac{\partial \vec{y}}{\partial z} \right) + \bar{Q} \quad (31)$$

or

$$\bar{B} \cdot \frac{\partial \vec{y}}{\partial t} = \vec{f}(\vec{y}, \vec{y}_z, \vec{y}_{zz}) \quad (32)$$

which is the general form of an 1D parabolic differential equation system. The initial and boundary conditions are

$$\vec{y}(t=t^0) = \vec{y}^0 \quad (33)$$

$$\bar{\alpha}_l \cdot \vec{y}_l + \bar{\beta}_l \cdot \frac{\partial \vec{y}}{\partial x} \Big|_l = \vec{\gamma}_l \quad (34)$$

$$\bar{\alpha}_r \cdot \vec{y}_r + \bar{\beta}_r \cdot \frac{\partial \vec{y}}{\partial x} \Big|_r = \vec{\gamma}_r. \quad (35)$$

In this notation \vec{y} is the vector of the state variables, *i.e.* the unknowns of the system with the dimension $m = 6$. \bar{B} , \bar{v} and \bar{D} are matrices with the dimension $(m \times m)$ and depend on \vec{y} , z and t . The vector \bar{Q} also depends on \vec{y} , z and t and has the same dimension as \vec{y} . $\bar{\alpha}$, $\bar{\beta}$ and $\bar{\gamma}$ are diagonal $(m \times m)$ matrices.

5 Solution of the model equations using a static grid

The system in Eqn. (31) along with Eqn. (33), (34) and (35) can be solved numerically using a method-of-lines (MOL) algorithm [35]. In this approach the space coordinate z is discretized such that the partial differential equations are transformed into a system of differential-algebraic equations (DAEs):

$$\bar{B}_i \cdot \frac{d\vec{y}_i}{dt} = \vec{f}_i(\vec{y}_i, \vec{y}_z|_i, \vec{y}_{zz}|_i) \quad i = 1, \dots, n \quad (36)$$

A finite difference method has been used for the discretization of the spatial domain throughout this paper. As described above the model can change at a specific coordinate z . Therefore, at each grid point it has to be checked if the surface is wet ($Y_M > 0$) or dry ($Y_M = 0$). For the dry parts the direction of the driving gradient for the water vapor transfer ($X_A - X_M$) has to be controlled.

For the solution of the DAEs one of the adaptive integration algorithms developed *e.g.* by Petzold [32] or Deuffhard [12, 13, 14] can be used. Another approach for the solution of Eqn. (31) is a fully adaptive MOL-treatment using regridding techniques such that both the spatial discretisation error and the error arising from the time integration [27, 28, 29] can be controlled. Nevertheless, the grid points along the space coordinate z are considered to be static in the following sense: The locations are fixed during one integration step. In this section this method is used as an example for a MOL-algorithm and will be discussed shortly below.

5.1 PDEXPACK – a fully adaptive solver for parabolic differential equations

The program package PDEXPACK has been developed recently to solve parabolic differential equations of the general form given in Eqn. (31). The program is based on the code PDEX [27] and allows the user to specify the equations to be solved in subroutines for the matrices \bar{B} , \bar{v} and \bar{D} and the vector \bar{Q} [16, 29]. The implemented method-of-lines discretization algorithm is suited for systems of parabolic differential equations ($\bar{D} \neq \bar{0}$). The dispersion term is necessary to get a satisfactory performance of PDEX (stability and suitable error control). Since a semi-implicit integration method is implemented in the code to handle stiff systems as well as systems with singular \bar{B} -matrix, the Jacobian matrix is required at each integration step.

The numerical algorithm is fully adaptive in time and space. The number of grid points necessary to achieve a certain accuracy for the approximated solution as well as the distribution of the grid points and the length of the time step are automatically adjusted by the program [29]. This adjustment is based upon the relative

errors for the time and the space discretization for every state variable at every gridpoint. These errors are estimated at each time step via extrapolation methods. The estimated local spatial errors are the base for a local regriding to equilibrate the error in the spatial domain. Based on the local error estimates global error norms are determined which allow for a separate error control in space and time.

The difficulties which arise for the present problem result from the fact that the equations to be solved may change from one spatial grid point to another and, at one specific gridpoint, during one integration step because of the step change function δ in Eqn. (11) - (16). This causes severe problems because the right hand side of Eqn. (36) is discontinuous. Furthermore the Jacobian matrix and the right hand side may not fit. Therefore, the performance of the extrapolation procedure, the error estimation and the stability properties are perturbed and the code works less efficient.

5.2 Simulation of evaporation from an initially wet matrix

Fig. 3 shows the results from a simulation which describes the evaporation from an initially wet matrix. At the beginning ($t = 0$ s) the matrix is wet over its whole length. The matrix temperature is kept constant during the entire simulation at $\vartheta_M = 20^\circ$ C. Corresponding to this temperature the saturated water content X_M at the matrix to air interface is constant at a value of approximately $15 \frac{\text{g}}{\text{kg}}$ which is also the initial profile for the water content X_A of the air. For all times $t > 0$ s a completely dry air stream with a temperature of $\vartheta_A = 40^\circ$ C enters the system at $z = 0$ m. It passes over the matrix with a velocity of $v_A = 4 \frac{\text{m}}{\text{s}}$ such that water is evaporating due to a difference between X_M and X_A . Therefore, the water content of the air increases along the space coordinate z whereas the matrix water content Y_M decreases with the simulation time. At the point where X_A reaches the value of the saturated water content X_M the transfer of water vapor stops.

As long as the matrix is wet (profiles ② and ③) the water content of the air does not change with the simulation time. As soon as the liquid water of the matrix is used up, a front with $Y_M = 0$ starts to move from the left to the right, *i.e.* a moving boundary is generated which separates the dry and the wet part of the matrix. The velocity of this front is much smaller than the flow velocity v_A of the air stream. At the end of the simulation ($t = 2.9$ s) the matrix is almost completely dry.

The example shows that PDEX is able to solve the problem above. The unsteady behaviour of the Jacobian matrix of the system near the grid point where the model equations switch yields a low grade of convergence of the solution method, small time steps during the integration and a high local grid point density near that point. A method how to overcome this problems will be discussed in the next sections.

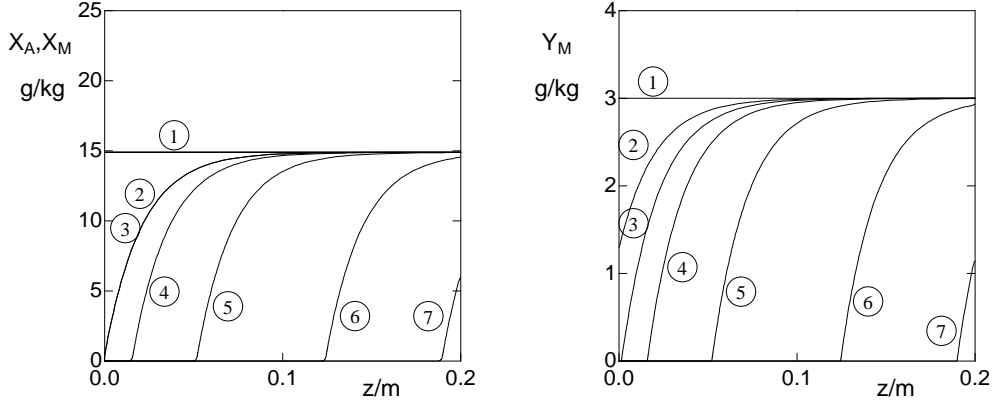


Figure 3: Evaporation from an initially wet matrix with constant matrix temperature: ① X_A, Y_M for $t = 0$ s and X_M for $t \geq 0$ s, ② $t = 0.16$ s, ③ $t = 0.3$ s, ④ $t = 0.5$ s, ⑤ $t = 1.0$ s, ⑥ $t = 2.0$ s, ⑦ $t = 2.9$ s.

6 Velocity of the moving boundary between wet and dry parts

The simulation results shown in Fig. 3 indicate that the boundary between the dry and the wet part of the matrix moves to the right with an almost constant velocity. If this velocity is known a priori, the moving boundary of the wet matrix can be localized such that the point where the model equations have to be switched can be determined in advance.

Fig. 4 gives a magnified view of an evaporation front moving to the right. The determination of the boundary moving velocity is just a special case of the general problem to determine the velocity v_M of the position of the constant water content Y_M . Out of several possibilities which all lead to the same result the case in Fig. 5 will be considered. Here dz and dt are chosen in such a way that the velocity v_M of a constant water content

$$Y_M^+ = Y_M(z, t) = Y_M(z + dz, t + dt) \quad (37)$$

can be written as

$$v_M = \frac{dz}{dt}. \quad (38)$$

A Taylor series expansion for Y_M yields

$$Y_M(z + dz, t + dt) = Y_M(z, t) + \frac{\partial Y_M}{\partial t} \cdot dt + \frac{\partial Y_M}{\partial z} \cdot dz + O(dz^2, dt^2) \quad (39)$$

Neglecting the terms of higher order the following expression for v_M results:

$$v_M = \frac{dz}{dt} = -\frac{\frac{\partial Y_M}{\partial t}}{\frac{\partial Y_M}{\partial z}} \quad (40)$$

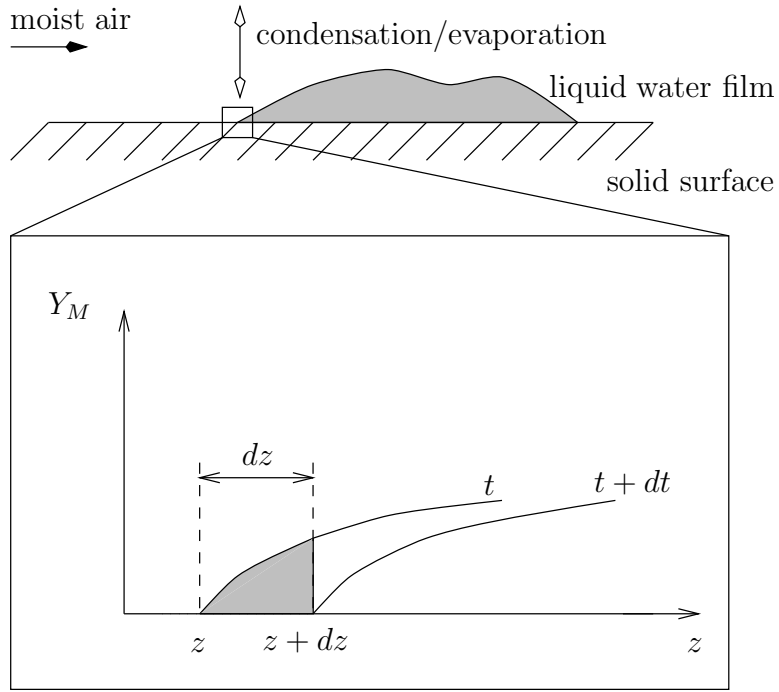


Figure 4: Moving boundary on the matrix

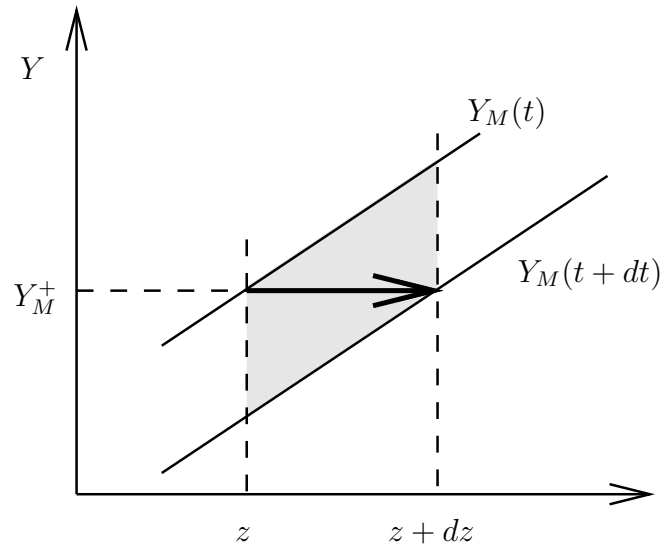


Figure 5: Moving front problem: Determination of the velocity v_M .

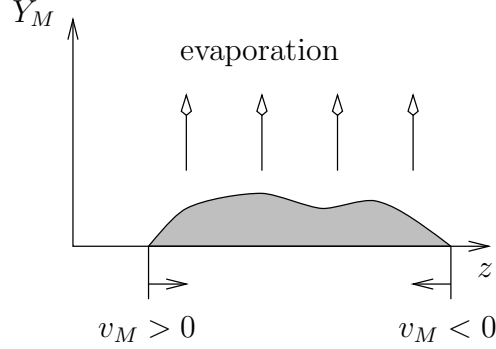


Figure 6: Moving boundaries due to evaporation

With Eqn. (13) for $\frac{\partial Y_M}{\partial t}$ the final result can be written as

$$v_M = \frac{a_V \cdot \beta \cdot (X_M - X_A)}{(1 - \varepsilon) \cdot \rho_S \cdot \frac{\partial Y_M}{\partial z}} \quad (41)$$

In the case of evaporation, *i.e.* $X_M > X_A$, the velocity v_M is positive if the spatial derivative is positive. If $\frac{\partial Y_M}{\partial z}$ becomes negative, the direction of the front changes and, accordingly, v_M in Eqn. (41) becomes negative, too. This is shown in Fig. 6.

7 Transformation to a moving coordinate system

Eqn. (41) can be used to position specific grid points exactly at the boundaries between the dry and the wet parts of the matrix. For the other grid points of the entire spatial domain it has to be decided, if either the equations for a wet (Eqn. (11) - (16) with $\delta = 1$) or a dry matrix ($\delta = 0$) apply. Now the model equations do not switch any more at one certain grid point and the right hand side is continuous and continuously differentiable. The problem using this method is that the selected moving grid points may cross static grid points. This can be handled with a special control strategy like the one used by Hasan et al. for the investigation of cyclic 1D melting and freezing [19]. If a moving grid point crosses a static grid point the two points change its features, *i.e.* the static grid point becomes a moving one and vice versa.

Another approach is that all grid points are assumed to be moving such that crossing cannot occur. Therefore, the changes of the state variables have to be described in a moving coordinate system. In Eqn. (31) the partial derivative $\frac{\partial \vec{y}}{\partial t}$ is the variation

of \vec{y} with time at a fixed position in the spatial domain whereas the total derivative

$$\frac{d\vec{y}}{dt} = \frac{\partial\vec{y}}{\partial t} + \frac{\partial\vec{y}}{\partial z} \cdot \frac{dz}{dt} \quad (42)$$

describes the change of \vec{y} with time while moving along the space coordinate with the velocity $w = \frac{dz}{dt}$ [3, 31]. By replacing the partial derivative Eqn. (31) can be rewritten as

$$\bar{B} \cdot \left(\frac{d\vec{y}}{dt} - w \cdot \frac{\partial\vec{y}}{\partial z} \right) = \vec{f}(\vec{y}, \vec{y}_z, \vec{y}_{zz}) \quad (43)$$

or

$$\bar{B} \cdot \frac{d\vec{y}}{dt} = \vec{f}(\vec{y}, \vec{y}_z, \vec{y}_{zz}) + \bar{B} \cdot w \cdot \frac{\partial\vec{y}}{\partial z} = \vec{g}(\vec{y}, \vec{y}_z, \vec{y}_{zz}) . \quad (44)$$

If the velocity w is equal to zero the partial derivative $\frac{\partial\vec{y}}{\partial t}$ coincides with the total derivative and Eqn. (44) and Eqn. (31) are equal.

Written in more detail, Eqns. (11) - (16) are transformed into the following system for moving coordinates (see [27] for more details):

$$\begin{aligned} \varepsilon \cdot \varrho_A \cdot \left(\frac{dX_A}{dt} - w \cdot \frac{\partial X_A}{\partial z} \right) &= -\varepsilon \cdot \varrho_A \cdot v_A \cdot \frac{\partial X_A}{\partial z} + \varepsilon \cdot D_{eff} \cdot \frac{\partial^2 X_A}{\partial z^2} \\ &\quad - \delta \cdot a_V \cdot \beta \cdot (X_A - X_M) \end{aligned} \quad (45)$$

$$0 = X_M - 0.622 \cdot \frac{p_W^{sat}(\vartheta_M)}{p - p_W^{sat}(\vartheta_M)} \quad (46)$$

$$(1 - \varepsilon) \cdot \varrho_S \cdot \left(\frac{dY_M}{dt} - w \cdot \frac{\partial Y_M}{\partial z} \right) = \delta \cdot a_V \cdot \beta \cdot (X_A - X_M) \quad (47)$$

$$\begin{aligned} \varepsilon \cdot \varrho_A \cdot c_p \cdot \left(\frac{d\vartheta_A}{dt} - w \cdot \frac{\partial\vartheta_A}{\partial z} \right) &= -\varepsilon \cdot \varrho_A \cdot v_A \cdot c_p \cdot \frac{\partial\vartheta_A}{\partial z} \\ &\quad + \varepsilon \cdot \lambda_{eff} \cdot \frac{\partial^2\vartheta_A}{\partial z^2} \\ &\quad - a_V \cdot \alpha \cdot (\vartheta_A - \vartheta_M) \end{aligned} \quad (48)$$

$$\begin{aligned} (1 - \varepsilon) \cdot \varrho_S \cdot c_M \cdot \left(\frac{d\vartheta_M}{dt} - w \cdot \frac{\partial\vartheta_M}{\partial z} \right) &= (1 - \varepsilon) \cdot \lambda_S \cdot \frac{\partial^2\vartheta_M}{\partial z^2} \\ &\quad + a_V \cdot \alpha \cdot (\vartheta_A - \vartheta_M) \\ &\quad + \delta \cdot a_V \cdot \beta \cdot (X_A - X_M) \\ &\quad \cdot (r_0 + c_{p,W} \cdot \vartheta_A - c_W \cdot \vartheta_M) \end{aligned} \quad (49)$$

$$\frac{\partial p}{\partial z} = -\frac{32 \cdot \nu \cdot \varrho_A \cdot v_A}{d_h^2} \quad (50)$$

For the case of a dry surface and $X_A < X_M$ ($\delta = 0$) the spatial derivative $\frac{\partial Y_M}{\partial z}$ vanishes and Eqn. (47) can be written as

$$(1 - \varepsilon) \cdot \varrho_S \cdot \frac{dY_M}{dt} = 0 \quad (51)$$

It would also be possible to solve the equation $Y_M = 0$, but Eqn. (51) is easier to implement.

8 Solution of the model equations using a moving grid

As in Sect. 5, the transformed partial differential Eqn. (44) can be solved using a method of lines algorithm like PDEXPACK. Because of the transformation to a moving coordinate system the ordinary differential equation (13) becomes a hyperbolic partial differential equation (47). Since PDEXPACK needs the stabilizing factor of a dispersion term [27], such a term is added arbitrarily to Eqn. (44) yielding

$$(1 - \varepsilon) \cdot \varrho_S \cdot \frac{dY_M}{dt} = (1 - \varepsilon) \cdot \varrho_S \cdot w \cdot \frac{\partial Y_M}{\partial z} + D_z \cdot \frac{\partial^2 Y_M}{\partial z^2} + a_V \cdot \beta \cdot (X_A - X_M) \quad (52)$$

The dispersion coefficient D_z is chosen such that the respective Péclet-number

$$Pe_z = \frac{(1 - \varepsilon) \cdot \varrho_S \cdot w \cdot L}{D_z} \quad (53)$$

has a minimum value of $Pe_z = 5000$. This ensures sufficient numerical stabilization while having negligible influence on the solution.

After spatial discretization Eqn. (43) transforms into

$$\bar{B}_i \cdot \left(\frac{d\vec{y}_i}{dt} - w_i \cdot \vec{y}_z|_i \right) = \vec{f}_i(\vec{y}_i, \vec{y}_z|_i, \vec{y}_{zz}|_i) \quad i = 1, \dots, n \quad (54)$$

or

$$\bar{B}_i \cdot \left(\frac{d\vec{y}_i}{dt} - \frac{dz_i}{dt} \cdot \vec{y}_z|_i \right) = \vec{f}_i(\vec{y}_i, \vec{y}_z|_i, \vec{y}_{zz}|_i) \quad i = 1, \dots, n. \quad (55)$$

Here w_i , the moving velocity of each grid point, has been replaced by $\frac{dz_i}{dt}$, because a grid point z_i moves by dz_i during on time step dt .

Since the location of the gridpoints change with time they can be considered as additional state variables. At each grid point z_i a new vector of unknowns $\tilde{\vec{y}}_i$ can be defined as

$$\tilde{\vec{y}}_i^T = (\vec{y}_i^T, z_i) \quad i = 1, \dots, n. \quad (56)$$

where

$$\tilde{y}_{i,m+1} = z_i. \quad (57)$$

The system of equations to be solved at each grid point can be written now as

$$\tilde{B}_i \cdot \frac{d\tilde{\vec{y}}_i}{dt} = \tilde{\vec{f}}_i(\tilde{\vec{y}}_i, \tilde{\vec{y}}_z|_i, \tilde{\vec{y}}_{zz}|_i). \quad (58)$$

Whereas the matrix \bar{B}_i in the discretized system (36) depends only on \vec{y}_i and z_i the matrix \tilde{B}_i in Eqn. (58) is now also a function of the state variables at the adjacent grid points z_{i-1} and z_{i+1} . This is due to the discretization formula of the spatial derivative $y_z|_i$ (see [29]) which is present in all equations in a product with the time derivative of the additional state variable $\tilde{y}_{i,m+1} = z_i$.

The additional equation for z_i can be obtained from the following considerations. In App. B it is shown how the error control algorithm of PDEXPACK has to be modified if the grid points move.

8.1 Grid points at boundaries of the spatial domain

The first and the last grid point of the spatial domain, *i.e.* z_1 and z_n , are not allowed to move. This leads to the following conditions:

$$\frac{dz_1}{dt} = 0 \quad (59)$$

$$\frac{dz_n}{dt} = 0 \quad (60)$$

8.2 Grid points at moving boundaries

To determine the position of the boundary between dry and wet parts of the matrix, a distinction should be made between evaporation and condensation. The evaporation case has been treated in Sect. 6 and resulted in an equation for the front moving velocity v_M (Eqn. (41)). If evaporation occurs ($X_A < X_M$) the position of the front is where Y_M changes from zero to positive values. If this position has been identified once it can be followed by the condition

$$\frac{dY_M}{dt} = 0 \quad (61)$$

The velocity v_M of this front has been derived as a special case in Sect. (6). It is interesting to note that the front moving velocity of an evaporation front (Eqn. (41)) can also be obtained from Eqn. (47) with Eqn. (61):

$$\frac{dz_k}{dt} = \frac{a_V \cdot \beta \cdot (X_M|_k - X_A|_k)}{(1 - \varepsilon) \cdot \varrho_S \cdot \left. \frac{\partial Y_M}{\partial z} \right|_k} = v_M$$

Examples will be discussed in Sect. 9.1 and 9.2.

If the matrix is dry ($Y_M = 0$) a second kind of moving boundary exists where the difference ($X_A - X_M$) changes its sign. Condensation starts as soon as X_A exceeds

X_M . Therefore, the front between a dry and a wet surface can be identified by the condition

$$0 = X_A - X_M. \quad (62)$$

This will be discussed in an example in Sect. 9.3 where the front moving velocity is not given by Eqn. 41.

It should be mentioned that following steep wave fronts, which is the aim of the moving grid algorithms *e.g.* proposed by Petzold [31], can be considered as a special case of the moving boundary problem discussed above. The condition $\frac{dy_j}{dt} = 0$ yields the velocity of one special grid point moving with the continuous front independently of the absolute value of y_j . In contrast to moving boundary problems the model equations do not change at this grid point.

8.3 Other grid points

For all other grid points the only requirement is that they do not cross each other. This is fulfilled if the ratio of the two adjacent grid point distances ($z_i - z_{i-1}$) and ($z_{i+1} - z_i$) stays constant while the grid points are moving. This is equivalent to the condition that the smoothness of the grid has to stay constant. For a grid with $z_{i-1} < z_i < z_{i+1}$ this can be expressed as

$$\frac{z_{i+1} - z_i}{z_i - z_{i-1}} \Big|_t = \frac{z_{i+1} - z_i}{z_i - z_{i-1}} \Big|_{t+dt}. \quad (63)$$

From the derivation in App. C it follows

$$\frac{w_{i+1} - w_i}{w_i - w_{i-1}} = \frac{z_{i+1} - z_i}{z_i - z_{i-1}} \quad (64)$$

such that the velocity $w_i = \frac{dz_i}{dt}$ can be expressed as a function of w_{i-1} and w_{i+1} .

With these assumptions the remainder of the missing equations is obtained:

$$\frac{z_{i+1} - z_i}{z_{i+1} - z_{i-1}} \cdot \frac{dz_{i-1}}{dt} + \frac{dz_i}{dt} + \frac{z_i - z_{i-1}}{z_{i+1} - z_{i-1}} \cdot \frac{dz_{i+1}}{dt} = 0 \quad 2 \leq i \leq k-1 \quad (65)$$

$$\frac{dz_k}{dt} = w_k \quad (66)$$

$$\frac{z_{i+1} - z_i}{z_{i+1} - z_{i-1}} \cdot \frac{dz_{i-1}}{dt} + \frac{dz_i}{dt} + \frac{z_i - z_{i-1}}{z_{i+1} - z_{i-1}} \cdot \frac{dz_{i+1}}{dt} = 0 \quad k+1 \leq i \leq n-1 \quad (67)$$

Eqn. (65) and (67) can be understood as a linear interpolation of the grid point velocities on the left and right side of grid point z_k . If no moving boundary is present the velocity w_k is zero and equal the velocity of all other grid points.

Eqn. (65)-(67) have been derived for one grid point z_k which moves with a moving boundary. In this case, the interpolation is carried out between the velocity of the boundary and zero which is the velocity at the ends of the spatial domain. There is no restriction for the number of moving boundaries to be considered since the same interpolation formulas can be used to compute the grid velocities between two moving boundaries.

It should be mentioned that in our example of a liquid water front on the matrix an explicit expression for w_k can be obtained (Eqn. (41)). In a more general case the velocity w_k may result from the numerical solution of the model equations and the additional condition at the grid point (compare the case of condensation on a dry matrix treated above).

9 Examples and performance of the moving grid method

This section shows the benefit of the moving grid algorithm compared to the method using a static grid discussed in Sect. 5.

9.1 Evaporation with one moving boundary

Fig. 7 shows the simulation of the evaporation from an initially wet matrix. Contrary to the example of Fig. 3 the matrix temperature ϑ_M changes during the simulation such that the corresponding saturated water content X_M changes, too. Dry air enters the regenerator from the left side at $z = 0$ with an inlet temperature of $\vartheta_A = 40^\circ \text{C}$ and is cooled by the matrix the initial temperature of which is $\vartheta_M = 20^\circ \text{C}$. Since the water content X_A is lower than the equilibrium value of the wet matrix X_M water evaporates into the air stream and the temperature of the matrix decreases because of the heat of evaporation. After 0.3s the matrix begins to dry out from the left side and the dry part is heated up by the warm air stream. A front with $Y_M = 0$ moves to the right and a moving boundary is generated.

Because of the switch from convective heating to (essentially) evaporative cooling before and after the evaporation front the matrix temperature exhibits a sharp bent at the front transition.

Fig. 8 illustrates how the velocity of the grid points is determined by the moving boundary. The depicted velocities correspond to the profiles shown in Fig. 7. As long as the whole matrix is wet no moving boundary exists and the grid points do not move (profiles ① and ②). As discussed in Sect. 8.1 the grid points at the inlet and outlet of the regenerator are fixed and the velocity of the front point moves with the velocity v_M . All other grid point velocities are determined by interpolation.

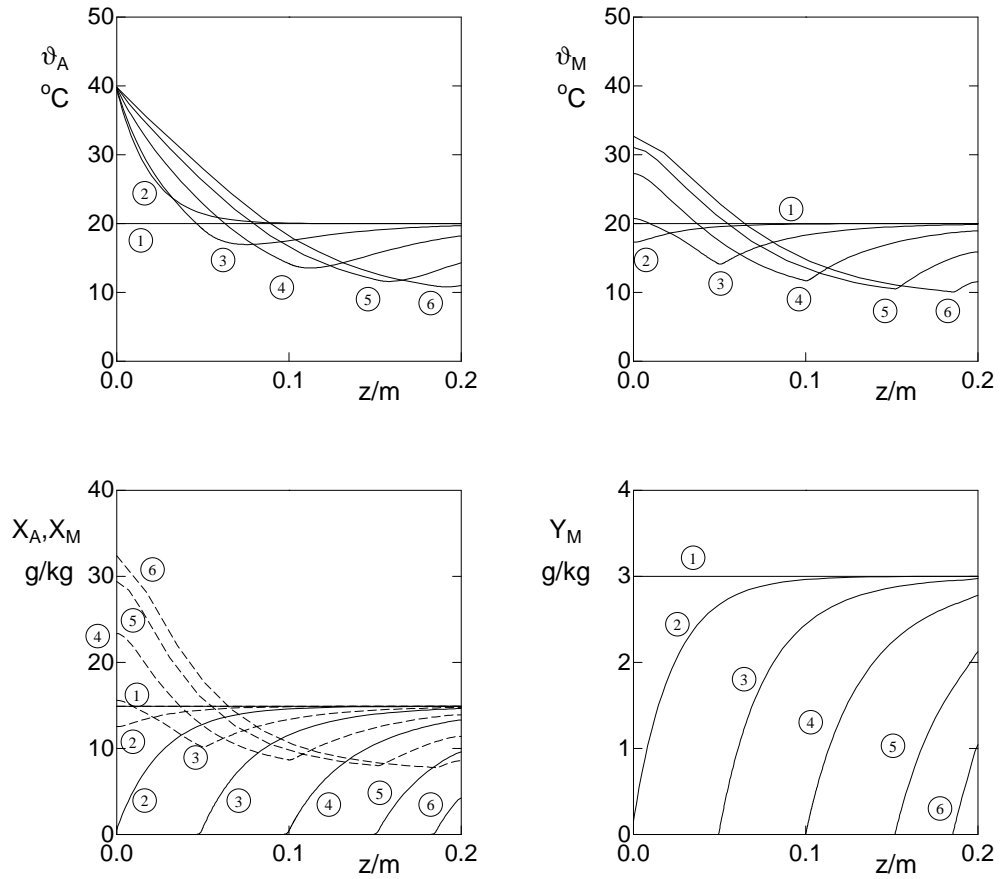


Figure 7: Evaporation from an initially wet matrix with varying matrix temperature: ① $t = 0\text{s}$, ② $t = 0.3\text{s}$ ③ $t = 0.9\text{s}$, ④ $t = 1.3\text{s}$, ⑤ $t = 2.1\text{s}$, ⑥ $t = 2.9\text{s}$, X_M (---), X_A (—).

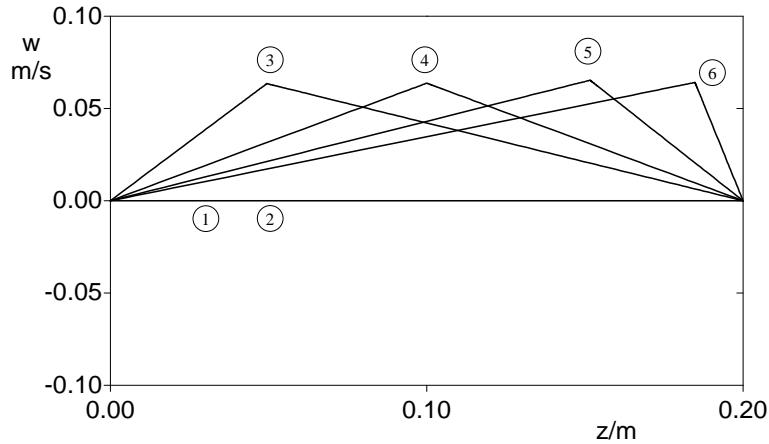


Figure 8: Velocity of the grid points with one moving boundary: ① $t = 0\text{s}$, ② $t = 0.3\text{s}$ ③ $t = 0.9\text{s}$, ④ $t = 1.3\text{s}$, ⑤ $t = 2.1\text{s}$, ⑥ $t = 2.9\text{s}$.

	Moving grid	Static grid
n_t	21	1114
\bar{n}_z	131	192
n_z^{min}	23	29
n_z^{max}	269	961
Stability	good	good
CPU-time [s]	25.5	1077.1

Table 1: Comparison of the performance for one moving boundary ($tol = 10^{-3}$)

	Moving grid ($Pe_z = \infty$)	Moving grid ($Pe_z = 5000$)	Static grid
n_t	23	17	250
\bar{n}_z	62	55	126
n_z^{min}	23	23	25
n_z^{max}	169	109	501
Stability	poor	good	poor
CPU-time [s]	13.6	9.2	126.1

Table 2: Comparison of the performance for one moving boundary ($tol = 5 \cdot 10^{-2}$)

The performance of the presented moving grid algorithm has been compared to the conventional method using a static grid. Tab. 1 and 2 show the number of time steps n_t and the average number of grid points \bar{n}_z . Because of the regriding techniques implemented in PDEXPACK the number of grid points is varying during the simulation between n_z^{min} and n_z^{max} . The required CPU-time for the simulations relates to a SPARC 5 workstation.

As illustrated in Tab. 1 both methods yield a stable solution for a specified error tolerance in time and space $tol = tol_t = tol_z = 10^{-3}$ (compare Eqn. (111) and (112) in App. B). However, compared to the moving grid the static grid algorithm requires much smaller time steps to correctly track the front. As discussed in Sect. 5 the right hand side becomes discontinuous at the point where the model equations have to be switched.

If the required tolerance is reduced to $tol = 5 \cdot 10^{-3}$ Tab. 2 indicates that a stable solution for the moving grid method cannot be obtained without the stabilizing factor of a (very small) dispersion term as discussed in Sect. 8. Compared to the performance with a more restrictive tolerance in Tab. 1 the number of selected time steps of the static grid method decreases by the factor four. Nevertheless, the low number of time steps of the moving grid method cannot be reached such that the

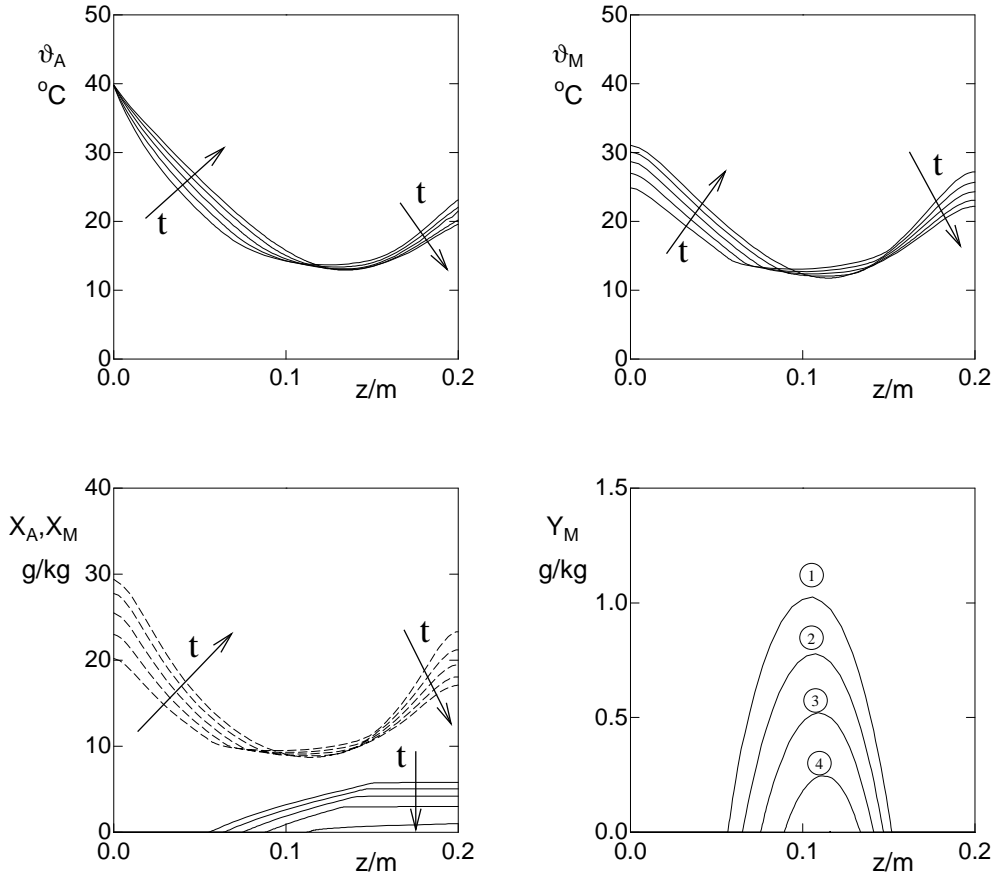


Figure 9: Evaporation during cyclic operation of a regenerator: ① $t = t^0$, ② $t = t^0 + 0.3s$, ③ $t = t^0 + 0.6s$, ④ $t = t^0 + 0.9s$, X_M (- - -), X_A (—).

required CPU-time is one order of magnitude higher for the static grid.

9.2 Evaporation with two moving boundaries

The example discussed above is not representative for situations which occur during the cyclic operation of an regenerative air to air heat exchanger. Instead of starting the simulation from a completely wetted matrix shown in Fig. 7 the profiles in Fig. 9 illustrate the period where a dry air stream enters the regenerator from the left end and the water content of the matrix Y_M at the beginning of the period is non-uniform (profile ①). Since the driving gradient for the transfer of water vapor is directed from the matrix to the air stream over the whole length of the matrix two moving boundaries are generated. During the simulation the water content X_A of the air stream increases only at that part of the matrix which is still wetted.

Fig. 10 shows that the velocities of the two grid points moving with the boundaries have opposite signs, *i.e.* the right moving boundary moves to the left which can also

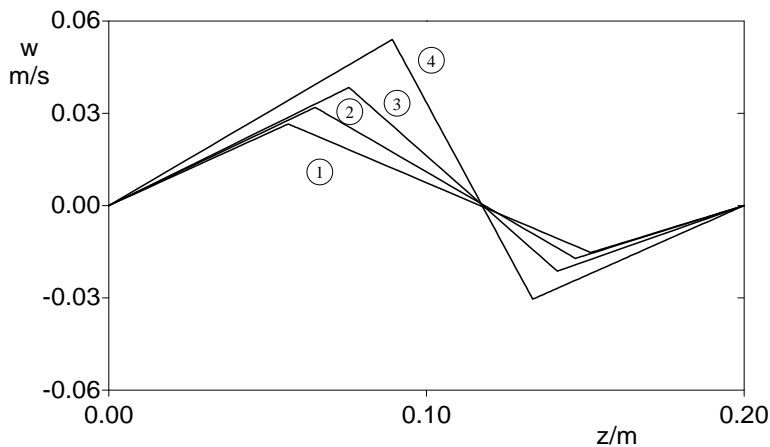


Figure 10: Velocity of the grid points with two moving boundaries: ① $t = t^0$, ② $t = t^0 + 0.3\text{s}$, ③ $t = t^0 + 0.6\text{s}$, ④ $t = t^0 + 0.9\text{s}$.

	Moving grid	Static grid
n_t	10	205
\bar{n}_z	204	219
n_z^{\min}	53	53
n_z^{\max}	329	469
Stability	good	good
CPU-time [s]	20.7	224

Table 3: Comparison of the performance for two moving boundaries with $tol = 10^{-3}$

be seen in Fig. 9 (profiles ② to ④).

The comparison of the performance between the moving and the static grid method is shown in Tab. 3. The gradients of the profiles in Fig. 9 are less steep than the ones in Fig. 7 such that both methods yield stable solutions without any stabilizing factors. Again the static grid method requires smaller time steps to achieve the specified accuracy such that for the moving grid method the computational effort is reduced by an order of magnitude.

9.3 Condensation on a dry matrix

The following example shows the phenomena which occur in a regenerative air to air heat exchanger if a moist air stream with $X_A = 14 \frac{g}{kg}$ and $\vartheta_M = 20^\circ C$ enters a dry and cold matrix with $\vartheta_M = 10^\circ C$. At the beginning of the simulation the air in the flow channels of the heat exchanger is completely dry. When the moist air stream enters from the left end, two different phenomena can be observed: condensation

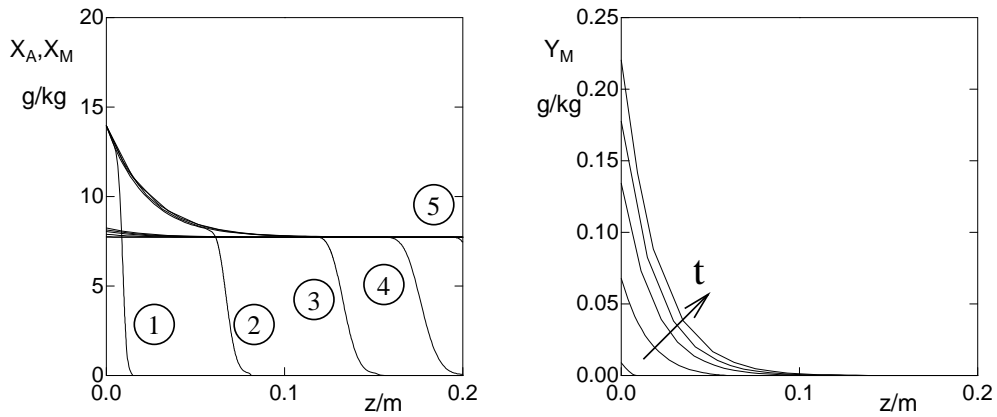


Figure 11: Condensation during cyclic operation of a regenerator: X_A , Y_M - ① $t = 0.002\text{s}$, ② $t = 0.015\text{s}$ ③ $t = 0.03\text{s}$, ④ $t = 0.04\text{s}$, ⑤ $t = 0.05\text{s}$. X_M is almost constant during the shown period. The matrix and the air in the regenerator were initially completely dry.

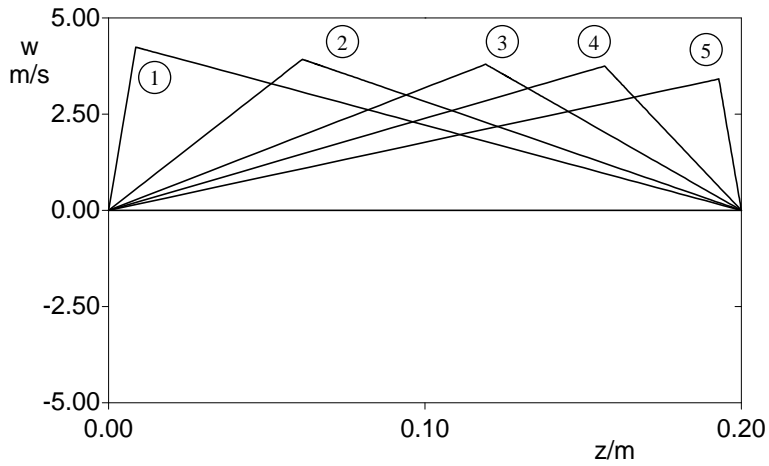


Figure 12: Velocity of the grid points with one moving boundary: ① $t = 0.002\text{s}$, ② $t = 0.015\text{s}$ ③ $t = 0.03\text{s}$, ④ $t = 0.04\text{s}$, ⑤ $t = 0.05\text{s}$.

	Moving grid	Static grid
n_t	26	44
\bar{n}_z	193	145
n_z^{min}	69	27
n_z^{max}	409	145
Stability	good	good
CPU-time [s]	46.7	20.6

Table 4: Comparison of the performance one moving boundary during condensation ($tol = 5 \cdot 10^{-3}$)

from the moist air stream onto the cold matrix and replacement of the dry air by the moist air.

In the simulation shown in Fig. 11 the velocity of the air is approximately $4 \frac{m}{s}$ such that the air has passed over the whole length of the matrix after 0.05s. During this small period of time the temperature of the matrix and therefore the saturation content can be considered to be constant at $X_M = 8 \frac{g}{kg}$ which is represented by the horizontal line in the left diagram of Fig. 11. This value is below the water content of the entering moist air such that condensation occurs onto the matrix at the left end and the water content of the moist air decreases (profile ①). After it drops below the saturation content of the matrix the condensation stops and the remaining part of the matrix remains dry and of course no evaporation can occur although the driving gradient is from the matrix to the dry air. While the dry air is displaced more and more the front moves towards the right end. The front of the moving boundary is now characterized by the identity $X_A = X_M$. This is in contrast to the examples of Sect. 9.1 and 9.2 where the moving boundaries are characterized by $Y_M = 0$ and the velocity v_M is determined by Eqn. (41). As discussed in Sect. 8 an explicit equation for a front with $X_A = X_M$ cannot be obtained. However, if the dispersion term is neglected, it can be seen from Eqn. (11) that a front with $X_A = X_M$ moves with the velocity v_A of the air stream which is much higher than the velocity for $Y_M = 0$ and shown in Fig. 12.

Tab. 4 shows the performance of the two solution methods for the example discussed above. Compared to the method using a static grid the moving grid algorithm requires only about half of the integration steps. Surprisingly, for the conventional algorithm with a static grid the number of grid points is smaller as well as the required CPU time. In the moving grid algorithm the point $X_A = X_M$ has to be determined during the simulation for $t < 0.05s$. Fig. 11 shows that there is a well defined intersection between X_A and X_M for the profiles ① and ②. Because of the asymptotic approach of X_A to X_M more and more grid points are required to characterize the identity $X_A = X_M$ accurately enough and the advantage of fewer

required time steps is compensated. The conventional static grid method shows disadvantages if the Jacobian matrix is unsteady which is the case for profile ① and ② with sharp intersection points. For the asymptotic approach of the profiles this disadvantage disappears and the performance of the moving grid method is poor due to the higher number of required grid points.

The example of condensation front movement on an originally dry surface has been treated above in some detail to show the general applicability of the method proposed. For practical purposes it would not be necessary to resolve the detailed changes within the first 0.05s of simulation. A pseudo-steady state assumption for the water vapor balance Eqn. 11 would be appropriate instead. The profile ⑤ in Fig. (12) would be the starting profile of this period.

10 Conclusions and open problems

A numerical method for solving 1D moving boundary problems arising from discontinuities has been presented. Compared to the conventional technique using a static grid the adaptive moving grid method is able to track the discontinuity in the governing model equations. Therefore, the equations do not switch during the simulation at any grid point such that the right hand side is continuous and larger time steps can be selected. This is shown in the simulations illustrating the evaporation in a regenerative air to air heat exchanger, even where more than one moving boundary is present. However, during the period of condensation, the moving grid method requires more grid points than the method using a static grid. This is due to the asymptotic approach of the profiles to the discontinuity and can be avoided with a pseudo steady state assumption for the gas phase. The derived method can also be applied for other 1D problems with moving boundaries arising in modelling of chemical engineering systems.

A still open problem is to find reliable, robust and accurate criteria for the first identification or disappearance of moving boundaries. A helpful tool could be the implementation of a so called dense output method which allows a continuous representation of the solution [18]. Furthermore, the development of efficient and reliable methods which allow a coupling of moving boundaries with geometrical fixed ones and the crossing of different moving boundaries is still an open question.

A Derivation of the balance equations

The following derivations apply for the control volume shown in Fig. 2.

A.1 Mass balance of the gas phase

Since air is considered to be non-condensable the mass balance equation for dry air is

$$\frac{\partial m_A}{\partial t} = -\frac{\partial \dot{m}_A}{\partial z} \cdot dz \quad (68)$$

Using $m_A = \varepsilon \cdot A \cdot \varrho_A \cdot dz$ and $\dot{m}_A = \varepsilon \cdot A \cdot \varrho_A \cdot v_A$ yields

$$\frac{\partial \varrho_A}{\partial t} = -\frac{\partial(\varrho_A \cdot v_A)}{\partial z} = -\varrho_A \cdot \frac{\partial v_A}{\partial z} - v_A \cdot \frac{\partial \varrho_A}{\partial z} \quad (69)$$

A.2 Mass balance of water vapor in the gas phase

The water vapor mass m_W is transferred through

- convection of vapor in the gas phase (\dot{m}_W^C),
- vapor transport between the phases ($d\dot{m}_W$) and
- dispersion of vapor in the gas phase (J_W)*.

This leads to the water vapor balance

$$\frac{\partial m_W}{\partial t} = -\frac{\partial \dot{m}_W^C}{\partial z} \cdot dz - \frac{\partial J_W}{\partial z} \cdot dz - d\dot{m}_W. \quad (70)$$

With $m_W = X_A \cdot m_A = X_A \cdot \varepsilon \cdot A \cdot \varrho_A \cdot dz$, $\dot{m}_W^C = X_A \cdot \dot{m}_A = X_A \cdot \varepsilon \cdot A \cdot \varrho_A \cdot v_A$, Fick's law of diffusion $J_W = -\varepsilon \cdot A \cdot D_{eff} \cdot \frac{\partial X_A}{\partial z}$ and insertion of Eqns. (69) and (8) in Eqn. (70) yields

$$\varepsilon \cdot \varrho_A \cdot \frac{\partial X_A}{\partial t} = -\varepsilon \cdot \varrho_A \cdot v_A \cdot \frac{\partial X_A}{\partial z} + \varepsilon \cdot D_{eff} \cdot \frac{\partial^2 X_A}{\partial z^2} - \beta \cdot a_V \cdot (X_A - X_M) \quad (71)$$

*Dispersive transport mechanisms (*e.g.* diffusion of mass or heat conduction) are usually neglected in the literature in the description of condensation and evaporation problems in rotary heat exchangers. However, the applied method should be valid for a wider class of processes *e.g.* in chemical reaction engineering, where dispersion effects can sometimes play a more significant role than in the example shown in this paper. Furthermore, using a dispersion coefficient enables to describe axial dispersion effects in the heat and mass balances due to radial temperature and water vapor distribution which takes into account the deviation from ideal plug flow behavior. Finally, the system of the governing equations should be parabolic for the solution algorithm used.

where a_V is the specific surface:

$$a_V = \frac{dA_S}{A \cdot dz} \quad (72)$$

The density of dry air ρ_A is determined by the ideal gas law:

$$\rho_A = \frac{M_A \cdot p}{R \cdot T_A} \quad \text{with} \quad T_A = \vartheta_A + 273.15 \quad (73)$$

A.3 Mass balance of liquid water on the matrix

The amount of water m_M^W on the matrix is considered to be fixed and can change only by mass transfer between the matrix and the air stream:

$$\frac{\partial m_M^W}{\partial t} = d\dot{m}_W \quad (74)$$

With $m_M^W = Y_M \cdot m_S = Y_M \cdot (1 - \varepsilon) \cdot \rho_S \cdot A \cdot dz$ and Eqn. (8) the following equation can be obtained:

$$(1 - \varepsilon) \cdot \rho_S \cdot \frac{\partial Y_M}{\partial t} = \beta \cdot a_V \cdot (X_A - X_M) \quad (75)$$

A.4 Energy balance of the gas phase

The internal energy U of the gas consisting of dry air and water vapor in the control volume changes because of

- convection and dispersion of enthalpy in the gas phase (\dot{H}),
- enthalpy transport with the water vapor between the phases ($h_W \cdot d\dot{m}_W$),
- heat flux between the phases ($d\dot{Q}$) and
- heat dispersion in the gas phase (J^T), described by Fourier's law of conduction.

It is assumed that the water vapor passes the phases boundary with the conditions of the flowing air. Therefore, the enthalpy of the flux between the phases is equal to the enthalpy h_W of the vapor in the moist air. With these assumptions and the application of the first law of thermodynamics on the control volume in Fig. 2 leads to the following balance equation:

$$\frac{\partial U}{\partial t} = -\frac{\partial \dot{H}}{\partial z} \cdot dz - \frac{\partial J^T}{\partial z} \cdot dz - h_W \cdot d\dot{m}_W - d\dot{Q}. \quad (76)$$

U will be replaced by

$$U = H - p \cdot V, \quad (77)$$

where the pressure p can be considered as pseudo-stationary. For an ideal gas the enthalpy of the gas phase can be calculated as the sum of the enthalpies of the species in the mixture:

$$H = m_A \cdot h_A + m_W \cdot h_W = m_A \cdot (h_A + X_A \cdot h_W) = m_A \cdot h \quad (78)$$

In the air stream enthalpy is transferred through convection and dispersion of water vapor:

$$\dot{H} = \dot{m}_A \cdot h + J_W \cdot h_W \quad (79)$$

The specific enthalpy $h = h_A + X_A \cdot h_W$ is based on the mass of dry air. With these correlations Eqn. (76) yields

$$\begin{aligned} \varepsilon \cdot A \cdot \varrho_A \cdot dz \cdot \frac{\partial h}{\partial t} + \varepsilon \cdot A \cdot h \cdot dz \cdot \frac{\partial \varrho_A}{\partial t} = & -\varepsilon \cdot A \cdot \varrho_A \cdot v_A \cdot \frac{\partial h}{\partial z} \cdot dz \\ & -\varepsilon \cdot A \cdot h \cdot \frac{\partial(\varrho_A \cdot v_A)}{\partial z} \cdot dz \\ & -J_W \cdot \frac{\partial h_W}{\partial z} \cdot dz - h_W \cdot \frac{\partial J_W}{\partial z} \cdot dz \\ & -\frac{\partial J^T}{\partial z} \cdot dz - h_W \cdot d\dot{m}_W - d\dot{Q}. \quad (80) \end{aligned}$$

With Fick's law of diffusion, Fourier's law of heat conduction

$$J^T = -\varepsilon \cdot A \cdot \lambda_{eff} \cdot \frac{\partial \vartheta_A}{\partial z}, \quad (81)$$

convective heat transfer between the matrix and the gas

$$d\dot{Q} = \alpha \cdot dA_s \cdot (\vartheta_A - \vartheta_M) \quad (82)$$

and inserting Eqn. (69) and (8) this simplifies to

$$\begin{aligned} \varepsilon \cdot \varrho_A \cdot \frac{\partial h}{\partial t} = & -\varepsilon \cdot \varrho_A \cdot v_A \cdot \frac{\partial h}{\partial z} + \varepsilon \cdot D_{eff} \cdot \frac{\partial X_A}{\partial z} \cdot \frac{\partial h_W}{\partial z} \\ & + \varepsilon \cdot D_{eff} \cdot h_W \cdot \frac{\partial^2 X_A}{\partial z^2} + \varepsilon \cdot \lambda_{eff} \cdot \frac{\partial^2 \vartheta_A}{\partial z^2} \\ & - h_W \cdot a_V \cdot \beta \cdot (X_A - X_M) - \alpha \cdot a_V \cdot (\vartheta_A - \vartheta_M). \quad (83) \end{aligned}$$

The specific enthalpy h depends on the temperature ϑ_A and the water content X_A of the air whereas the specific enthalpy h_W of the water vapor depends only of the temperature. As a reference point for the enthalpy usually the temperature $\vartheta^0 = 0^\circ \text{C}$ is chosen [36]:

$$h = c_{p,A} \cdot \vartheta_A + X_A \cdot (r_0 + c_{p,W} \cdot \vartheta_A) \quad (84)$$

$$h_W = r_0 + c_{p,W} \cdot \vartheta_A \quad (85)$$

The specific heat capacities $c_{p,A}$ and $c_{p,W}$ are assumed to be constant. The differentials are obtained after applying the product rule:

$$\frac{\partial h}{\partial t} = (c_{p,A} + X_A \cdot c_{p,W}) \cdot \frac{\partial \vartheta_A}{\partial t} + (r_0 + c_{p,W} \cdot \vartheta_A) \cdot \frac{\partial X_A}{\partial t} \quad (86)$$

$$\frac{\partial h}{\partial z} = (c_{p,A} + X_A \cdot c_{p,W}) \cdot \frac{\partial \vartheta_A}{\partial z} + (r_0 + c_{p,W} \cdot \vartheta_A) \cdot \frac{\partial X_A}{\partial z} \quad (87)$$

$$\frac{\partial h_W}{\partial z} = c_{p,W} \cdot \frac{\partial \vartheta_A}{\partial z} \quad (88)$$

The enthalpy changes in Eqn. (83) can be replaced by these correlations such that the following energy balance for the gas phase can be obtained:

$$\begin{aligned} \varepsilon \cdot \varrho_A \cdot (c_{p,A} + X_A \cdot c_{p,W}) \cdot \frac{\partial \vartheta_A}{\partial t} + \\ \varepsilon \cdot \varrho_A \cdot (r_0 + c_{p,W} \cdot \vartheta_A) \cdot \frac{\partial X_A}{\partial t} = & -\varepsilon \cdot \varrho_A \cdot v_A \cdot (c_{p,A} + X_A \cdot c_{p,W}) \cdot \frac{\partial \vartheta_A}{\partial z} \\ & -\varepsilon \cdot \varrho_A \cdot v_A \cdot (r_0 + c_{p,W} \cdot \vartheta_A) \cdot \frac{\partial X_A}{\partial z} \\ & +\varepsilon \cdot D_{eff} \cdot \frac{\partial X_A}{\partial z} \cdot c_{p,W} \cdot \frac{\partial \vartheta_A}{\partial z} \\ & +\varepsilon \cdot D_{eff} \cdot (r_0 + c_{p,W} \cdot \vartheta_A) \cdot \frac{\partial^2 X_A}{\partial z^2} \\ & +\varepsilon \cdot \lambda_{eff} \cdot \frac{\partial^2 \vartheta_A}{\partial z^2} \\ & -\beta \cdot a_V \cdot (r_0 + c_{p,W} \cdot \vartheta_A) \cdot (X_A - X_M) \\ & -\alpha \cdot a_V \cdot (\vartheta_A - \vartheta_M) \end{aligned} \quad (89)$$

Inserting the mass balance of Eqn. (71) yields

$$\begin{aligned} \varepsilon \cdot \varrho_A \cdot c_p \cdot \frac{\partial \vartheta_A}{\partial t} = & -\varepsilon \cdot \varrho_A \cdot v_A \cdot c_{p,W} \cdot \frac{\partial \vartheta_A}{\partial z} + \varepsilon \cdot D_{eff} \cdot c_{p,W} \cdot \frac{\partial X_A}{\partial z} \cdot \frac{\partial \vartheta_A}{\partial z} \\ & +\varepsilon \cdot \lambda_{eff} \cdot \frac{\partial^2 \vartheta_A}{\partial z^2} - a_V \cdot \alpha \cdot (\vartheta_A - \vartheta_M) \end{aligned} \quad (90)$$

with

$$c_p = c_{p,A} + X_A \cdot c_{p,W}. \quad (91)$$

It may be surprising that that transfer of water vapor between the phases does not affect the temperature ϑ_A of the air. This is due to the assumption that water vapor passes the phase boundary with the state of the air stream. The phase changes like evaporation or condensation take place on the matrix.

A.5 Energy balance of the matrix

The internal energy of the matrix consisting of solid material and a water film changes because of the heat flux and the enthalpy transport with the flux of water

vapor between the air stream and the matrix. In the solid part of the matrix, axial conduction of heat (flux J_M^T) is considered:

$$\frac{\partial U_M}{\partial t} = -\frac{\partial J_M^T}{\partial z} \cdot dz + h_W \cdot dm_W + d\dot{Q} \quad (92)$$

The energy of the wet matrix can be calculated as the sum of the energy of the solid part and the energy of the liquid water:

$$U_M = m_S \cdot u_S + m_W \cdot u_W = m_S \cdot (u_S + Y_M \cdot u_W) = m_S \cdot u \quad (93)$$

With Fourier's law of heat conduction $J_M^T = -(1 - \varepsilon) \cdot A \cdot \lambda_S \cdot \frac{\partial \vartheta_M}{\partial z}$ and inserting Eqn. (82),(8) this leads to

$$(1 - \varepsilon) \cdot \varrho_S \cdot \frac{\partial u}{\partial t} = (1 - \varepsilon) \cdot \lambda_S \frac{\partial^2 \vartheta_M}{\partial z^2} + h_W \cdot \beta \cdot a_V \cdot (X_A - X_M) + \alpha \cdot a_V \cdot (\vartheta_A - \vartheta_M). \quad (94)$$

The specific energy $u = u_S + Y_M \cdot u_W$ depends on the temperature ϑ_M and the water content Y_M . As a reference point again the temperature $\vartheta^0 = 0^\circ \text{C}$ is chosen [36] and the specific heat capacities c_S and c_W are assumed to be constant:

$$u = c_S \cdot \vartheta_M + Y_M \cdot c_W \cdot \vartheta_M \quad (95)$$

The change of the internal energy can be expressed as

$$\frac{\partial u}{\partial t} = (c_S + Y_M \cdot c_W) \cdot \frac{\partial \vartheta_M}{\partial t} + c_W \cdot \vartheta_M \cdot \frac{\partial Y_M}{\partial t} \quad (96)$$

With these expressions Eqn. (94) can be written as

$$\begin{aligned} (1 - \varepsilon) \cdot \varrho_S \cdot (c_S + Y_M \cdot c_W) \cdot \frac{\partial \vartheta_M}{\partial t} + \\ (1 - \varepsilon) \cdot \varrho_S \cdot c_W \cdot \vartheta_M \cdot \frac{\partial Y_M}{\partial t} = (1 - \varepsilon) \cdot \lambda_S \frac{\partial^2 \vartheta_M}{\partial z^2} \\ + (r_0 + c_{p,W} \cdot \vartheta_A) \cdot a_V \cdot \beta \cdot (X_A - X_M) \\ + \alpha \cdot a_V \cdot (\vartheta_A - \vartheta_M). \end{aligned} \quad (97)$$

Inserting the mass balance in Eqn. (75) yields

$$\begin{aligned} (1 - \varepsilon) \cdot \varrho_S \cdot c_M \cdot \frac{\partial \vartheta_M}{\partial t} = (1 - \varepsilon) \cdot \lambda_S \cdot \frac{\partial^2 \vartheta_M}{\partial z^2} + a_V \cdot \alpha \cdot (\vartheta_A - \vartheta_M) \\ + a_V \cdot \beta \cdot (X_A - X_M) \\ \cdot (r_0 + c_{p,W} \cdot \vartheta_A - c_W \cdot \vartheta_M) \end{aligned} \quad (98)$$

with

$$c_M = c_S + Y_M \cdot c_W \quad (99)$$

The last term in Eqn. (98) describes the temperature change of the matrix due to condensation and evaporation. It contains the total difference between the enthalpy of water vapor and enthalpy of liquid water on the matrix.

A.6 Momentum balance

Instead of a dynamic momentum balance a pseudo-stationary pressure drop equation for laminar flow is used throughout this paper to compute the pressure along the flow length of the regenerative heat exchanger:

$$\frac{\partial p}{\partial z} = - \frac{32 \cdot \nu \cdot \rho_A \cdot v_A}{d_h^2} \quad (100)$$

A.7 Boundary Conditions

For the partial differential equations boundary conditions have to be specified. For the energy balance of the matrix it is assumed that the boundaries are adiabatic:

$$\left. \frac{\partial \vartheta_M}{\partial z} \right|_{z=0} = 0 \quad (101)$$

$$\left. \frac{\partial \vartheta_M}{\partial z} \right|_{z=L} = 0 \quad (102)$$

For the mass and energy balance of the gas the boundary conditions are derived with the assumption that axial dispersion of mass and heat is limited to the inside of the heat exchanger and can be neglected outside. The procedure corresponds to the derivation of the common Danckwerts Boundary Conditions [11]. The boundary conditions have to be switched depending on the flow direction of the air. If the air stream enters the heat exchanger from the left end a mass balance for water vapor at the inlet at $z = 0$ yields

$$D_{eff} \cdot \left. \frac{\partial X_A}{\partial z} \right|_{z=0} = \rho_A \cdot v_A \cdot [X_A(z=0) - X_A^*] \quad (103)$$

At the outlet of the regenerator the dispersion can be neglected.

$$\left. \frac{\partial X_A}{\partial z} \right|_{z=L} = 0. \quad (104)$$

The energy balance at the inlet of the heat exchanger yields

$$\dot{m}_A \cdot h^* = \dot{m}_A \cdot h(z=0) - h_W(z=0) \cdot \varepsilon \cdot A \cdot D_{eff} \cdot \left. \frac{\partial X_A}{\partial z} \right|_{z=0} - \varepsilon \cdot A \cdot \lambda_{eff} \cdot \left. \frac{\partial \vartheta_A}{\partial z} \right|_{z=0} \quad (105)$$

With Eqn. (84),(85) and (22) this can be written as

$$\begin{aligned} \dot{m}_A \cdot [c_{p,A} \cdot \vartheta_A^* + X_A^* \cdot (r_0 + c_{p,W} \cdot \vartheta_A^*)] = \\ \dot{m}_A \cdot [c_{p,A} \cdot \vartheta_A(z=0) + X_A(z=0) \cdot (r_0 + c_{p,W} \cdot \vartheta_A(z=0))] \\ - \dot{m}_A \cdot [r_0 + c_{p,W} \cdot \vartheta_A(z=0)] \cdot [X_A(z=0) - X_A^*] \\ - \varepsilon \cdot A \cdot \lambda_{eff} \cdot \left. \frac{\partial \vartheta_A}{\partial z} \right|_{z=0} \end{aligned} \quad (106)$$

or

$$\begin{aligned} \dot{m}_A \cdot c_{p,A} \cdot [\vartheta_A^* - \vartheta_A(z=0)] + \dot{m}_A \cdot c_{p,W} \cdot X_A^* \cdot [\vartheta_A^* - \vartheta_A(z=0)] \\ = -\varepsilon \cdot A \cdot \lambda_{eff} \cdot \left. \frac{\partial \vartheta_A}{\partial z} \right|_{z=0} \end{aligned} \quad (107)$$

Therefore, the boundary conditions for the energy balance of the gas phase are

$$\lambda_{eff} \cdot \left. \frac{\partial \vartheta_A}{\partial z} \right|_{z=0} = \varrho_A \cdot v_A \cdot (c_{p,A} + X_A^* \cdot c_{p,W}) \cdot (\vartheta_A(z=0) - \vartheta_A^*) \quad (108)$$

$$\left. \frac{\partial \vartheta_A}{\partial z} \right|_{z=L} = 0. \quad (109)$$

The pressure at the inlet is fixed such that

$$p(z=0) = p^*. \quad (110)$$

B Scaling and weighting for error control

The error control implemented in PDEXPACK is based on relative error criterions. An integration step is only accepted if the relative global error norms ε_t and ε_z fulfill the conditions

$$\varepsilon_t \leq tol_t \quad (111)$$

$$\varepsilon_z \leq tol_z \quad (112)$$

where tol_t and tol_z are user specified error tolerances. The error norms are computed out from relative errors for every state variable at every gridpoint. Therefore, the estimated absolute error $\Delta y_j(t, z_i)$ of each state variable y_j has to be weighted with a suitable weighting factor[16, 30]:

$$\varepsilon_j(t, z_i) = \frac{\Delta y_j(t, z_i)}{\psi_j(t, z_i)} \quad (113)$$

where $\vec{\psi}(t, z_i)$ is chosen such that

$$\psi_j(t, z_i) = \max\left(y_j(t, z_i), y_j^{thresh}\right). \quad (114)$$

The value y_j^{thresh} determines a lower threshold for the accuracy and divisions by zero can be prevented. If $y_j(t, z_i) > y_j^{thresh}$ a true relative error is estimated, if $y_j(t, z_i) < y_j^{thresh}$ an absolute error is estimated.

This procedure for the error determination cannot be applied for the vector \vec{y} which contains the moving grid points z_i as state variables. Using the relative error from

Eqn. (113) and (114) grid points at the left end of the spatial domain are computed with a higher accuracy than grid points at the right end. Since the accuracy for the moving grid points should be the same for the whole spatial domain the following relation for the determination of the errors of the grid points has been implemented in PDEXPACK:

$$\varepsilon_j(t, z_i) = \frac{\Delta z_i(t)}{z^{thresh}} \quad (115)$$

C Determination of the grid velocity

For the grid points $z_{i-1} < z_i < z_{i+1}$ the following condition must be fulfilled:

$$\left. \frac{z_{i+1} - z_i}{z_i - z_{i-1}} \right|_t = \left. \frac{z_{i+1} - z_i}{z_i - z_{i-1}} \right|_{t+dt} \quad (116)$$

With

$$z_l(t + dt) = z_l(t) + w_l(t) \cdot dt \quad l = i - 1, i, i + 1 \quad (117)$$

this can be expressed as

$$\frac{z_{i+1}(t) - z_i(t)}{z_i(t) - z_{i-1}(t)} = \frac{z_{i+1}(t) + w_{i+1}(t) \cdot dt - z_i(t) - w_i(t) \cdot dt}{z_i(t) + w_i(t) \cdot dt - z_{i-1}(t) - w_{i-1}(t) \cdot dt}. \quad (118)$$

For simplicity the dependence from t can be omitted such that

$$\frac{z_{i+1} - z_i}{z_i - z_{i-1}} = \frac{(z_{i+1} - z_i) + (w_{i+1} - w_i) \cdot dt}{(z_i - z_{i-1}) + (w_i - w_{i-1}) \cdot dt} \quad (119)$$

and

$$\frac{w_{i+1} - w_i}{w_i - w_{i-1}} = \frac{z_{i+1} - z_i}{z_i - z_{i-1}} \quad (120)$$

is obtained which is the same as Eqn. (64).

Notation

Letters	Unit	
A	m^2	area
a_V	$\frac{\text{m}^2}{\text{m}^3}$	geometrical surface to volume ratio
\bar{B}	div	matrix of storage

c_p	$\frac{\text{J}}{\text{kg}\cdot\text{K}}$	gas heat capacity
c_S	$\frac{\text{J}}{\text{kg}\cdot\text{K}}$	solid heat capacity
c_W	$\frac{\text{J}}{\text{kg}\cdot\text{K}}$	heat capacity of liquid water
c	$\frac{\text{mol}}{\text{m}^3}$	concentration
D_{eff}	$\frac{\text{kg}\cdot\text{m}^2}{\text{s}}$	dispersion coefficient
D	$\frac{\text{m}}{\text{s}}$	diffusion coefficient
d_h	m	hydraulic diameter
\bar{D}	div	matrix of dispersive transport
\vec{f}	div	vector of right hand side
\vec{g}	div	vector of modified right hand side after transformation
H	J	enthalpie
h	$\frac{\text{J}}{\text{kg}}$	specific enthalpy
\dot{H}	$\frac{\text{J}}{\text{s}}$	enthalpie flux
J^T	W	heat flux by conduction
J_W	$\frac{\text{kg}}{\text{s}}$	water vapor flux by diffusion
L	m	length
M	$\frac{\text{kg}}{\text{mol}}$	molar weight
m	-	number of unknowns
m	kg	mass
\dot{m}	$\frac{\text{kg}}{\text{s}}$	mass flux
n_z	-	number of gridpoints
n_z	-	number of timesteps
\dot{n}	$\frac{\text{mol}}{\text{m}^2\cdot\text{s}}$	mole flux per area
p	Pa	pressure
Pe	-	Peclet number
\vec{Q}	div	vector of source terms
\dot{Q}	W	heat
R	$\frac{\text{J}}{\text{mol}\cdot\text{K}}$	gas constant
r	m	radial coordinate
r_0	$\frac{\text{J}}{\text{kg}}$	enthalpy of evaporation
T	K	temperature
t	s	independent variable (time)
tol	-	tolerance
U	J	internal energy
u	$\frac{\text{J}}{\text{kg}}$	specific internal energy
V	m^3	volume
v	$\frac{\text{m}}{\text{s}}$	velocity
w	$\frac{\text{m}}{\text{s}}$	velocity of moving grid points
X_A	$\frac{\text{kg}_{\text{water vapor}}}{\text{kg}_{\text{dry air}}}$	water content in dry air
X_M	$\frac{\text{kg}_{\text{water vapor}}}{\text{kg}_{\text{dry air}}}$	water content in equilibrium

Y_M	$\frac{\text{kg}_{\text{liquid water}}}{\text{kg}_{\text{matrix}}}$	with matrix temperature
\vec{y}	div	water content of the matrix
\tilde{y}	div	vector of dependent state variables
		vector of dependent state variables
		in moving system
z	m	independent variable (space coordinate)

Greek letters Unit

α	$\frac{\text{W}}{\text{m}^2 \cdot \text{K}}$	heat transport coefficient
$\bar{\alpha}$	div	diagonal - matrix of
		boundary condition coefficients
β	$\frac{\text{m}}{\text{s}}$	mass transport coefficient
$\bar{\beta}$	div	diagonal - matrix of
		boundary condition coefficients
$\bar{\gamma}$	div	diagonal - matrix of
		boundary condition coefficients
Δ	-	difference
δ	-	step change function
ε_t	div	error estimate in time
ε_z	div	error estimate in space
ε	-	void fraction
λ	$\frac{\text{W}}{\text{m} \cdot \text{K}}$	thermal conductivity
ν	$\frac{\text{m}^2}{\text{s}}$	viscosity
$\vec{\Psi}$	div	vector of weighting factors
ϱ	$\frac{\text{kg}}{\text{m}^3}$	density
ϑ	$^{\circ}\text{C}$	temperature

Upper indices

C	convection
max	maximum
min	minimum
sat	saturation
$thresh$	threshold
W	water
0	initial conditions
$*$	inlet

Lower indices

A	dry air
i	index of gridpoints
j	index of state variables
k	special grid point
l	left boundary
M	matrix
r	right boundary
S	solid
W	water

References

- [1] T. Ahn, W. V. Pinczewski and D. L. Trimm. Transient Performance of Catalytic Combustors for Gas Turbine Applications. *Chemical Engineering Science*, 41(1):55–64, 1986.
- [2] ASHREA. Handbook of Fundamentals. American Society of Heating, Refrigeration and Air Conditioning Engineers, 1984.
- [3] R. B. Bird, W. E. Stewart and E. N. Lightfoot. *Transport Phenomena*. John Wiley and Sons, 1960.
- [4] K. B. Bischoff. Accuracy of the Pseudo Steady State Approximation for Moving Boundary Diffusion Problems. *Chemical Engineering Science*, 18:711–713, 1963.
- [5] J. G. Blum, J. M. Sanz-Serna and J. G. Verwer. On Simple Moving Grid Methods for One-Dimensional Evolutionary Partial Differential Equations. *Journal of Computational Physics*, 74:191–213, 1988.
- [6] H. J. H. Brouwers. An Improved Tangency Condition for Fog Formation in Cooler-Condensers. *International Journal of Heat and Mass Transfer*, 34(9):2387–2394, 1991.
- [7] H. J. H. Brouwers. A Film Model for Heat and Mass Transfer with Fog Formation. *Chemical Engineering Science*, 47(12):3023–3036, 1992.
- [8] H. J. H. Brouwers. Film Models for Transport Phenomena with Fog Formation: The Fog Film Model. *International Journal of Heat and Mass Transfer*, 35(11):13–28, 1992.

- [9] H. J. H. Brouwers and A. K. Chesters. Film Models for Transport Phenomena with Fog Formation: The Classical Film Model. *International Journal of Heat and Mass Transfer*, 35(11):1–11, 1992.
- [10] H. J. H. Brouwers and C. W. M. van der Geld. Heat Transfer, Condensation and Fog Formation in Crossflow Plastic Heat Exchangers. *International Journal of Heat and Mass Transfer*, 39(2):391–405, 1996.
- [11] P. V. Danckwerts. Continuous flow systems. *Chemical Engineering Science*, 2(1):1–13, 1953.
- [12] P. Deuffhard. Order and Stepsize Control in Extrapolation Methods. *Numerische Mathematik*, 41:399–422, 1983.
- [13] P. Deuffhard, E. Hairer and J. Zugk. One-step and Extrapolation Methods for Differential Algebraic Systems. *Numerische Mathematik*, 51:501–515, 1987.
- [14] P. Deuffhard, U. Nowak and M. Wulkow. Recent Developments in Chemical Computing. *Computers and Chemical Engineering*, 14(11):1249–1258, 1990.
- [15] M. Epstein and D. E. Rosner. Enhancement of Diffusion-Limited Vaporization Rates by Condensation within the Thermal Boundary Layer - 2. Comparison of Homogeneous Nucleation Theory with the Critical Supersaturation Model. *International Journal of Heat and Mass Transfer*, 13:1393–1414, 1970.
- [16] J. Frauhammer. Numerische Lösung von eindimensionalen parabolischen Systemen mit adaptiven Gittern. Diplomarbeit am Institut für Chemische Verfahrenstechnik, Universität Stuttgart, 1992.
- [17] R. M. Furzeland, P. A. Verwer and A. Zegeling. A Numerical Study of Three Moving Grid Methods for One-Dimensional Partial Differential Equations which are Based on the Method of Lines. *Journal of Computational Physics*, 89(349-388), 1990.
- [18] E. Hairer and A. Ostermann. Dense Output for Extrapolation Methods. *Numerical Mathematics*, 58:419–439, 1990.
- [19] M. Hasan, A. S. Mujumdar and M. E. Weber. Cyclic Melting and Freezing. *Chemical Engineering Science*, 46(7):1573–1587, 1991.
- [20] H. Hausen. Wärmeübertragung im Gegenstrom, Gleichstrom und Kreuzstrom. Springer Verlag, 1st edition, 1970.
- [21] Y. Hayashi, A. Takimoto and M. Kanbe. Transport-Reaction Mechanism of Mist Formation Based on the Critical Supersaturation Model. *Transactions of the ASME: Journal of Heat Transfer*, pages 114–119, February 1976.

- [22] R. B. Holmberg. Heat and Mass Transfer in Regenerators with Nonhygroscopic Rotor Materials. *Transactions of the ASME: Journal of Heat Transfer*, 99(5):196–202, 1977.
- [23] W. M. Kays and A. L. London. *Compact Heat Exchangers*. McGraw Hill Book Company, 3rd edition, 1984.
- [24] F. Legay-Desequelles and B. Prunet-Foch. Dynamic Behaviour of a Boundary Layer with Condensation along a Flat Plate: Comparison with Suction. *International Journal of Heat and Mass Transfer*, 28(12):2363–2370, 1985.
- [25] F. Legay-Desequelles and B. Prunet-Foch. Heat and Mass Transfer with Condensation in Laminar and Turbulent Boundary Layers along a Flat Plate. *International Journal of Heat and Mass Transfer*, 29(1):95–105, 1986.
- [26] H. Martin. *Wärmeübertrager*. Georg Thieme Verlag, 1st edition, 1988.
- [27] U. Nowak. Adaptive Linienmethoden für parabolische Systeme in einer Raumdimesion, TR 93-14. Technical report, Konrad-Zuse-Zentrum für Informationstechnik, Berlin, 1993.
- [28] U. Nowak. A Fully Adaptive MOL-Treatment of Parabolic 1-D Problems with Extrapolation Techniques. *Applied Numerical Mathematics*, 20:129–145, 1996.
- [29] U. Nowak, J. Frauhammer and U. Nieken. A Fully Adaptive Algorithm for Parabolic Differential Equations in One Space Dimesion. *Computers and Chemical Engineering*, 20(5):547–561, 1996.
- [30] U. Nowak and L. Weimann. A Family of Newton Codes for Systems of Highly Nonlinear Equations, TR 91-10. Technical report, Konrad Zuse Zentrum für Informationstechnik, 1991.
- [31] L. Petzold. Observations on an Adaptive Moving Grid Method for One-Dimensional Systems of Partial Differential Equations. *Applied Numerical Mathematics*, 3:347 – 360, 1987.
- [32] L. R. Petzold. A Description of DASSL: A Differential / Algebraic System Solver, volume 3. *Scientific Computing*, ed. R.S. Stepleman et al., Elsevier, 1983.
- [33] J. I. Ramos. Adaptive Methods of Lines for One-Dimensional Reaction-Diffusion Equations. *International Journal for Numerical Methods in Fluids*, 16:697–723, 1993.
- [34] D. E. Rosner. Enhancement of Diffusion-Limited Vaporization Rates by Condensation within the Thermal Boundary Layer: 1. The Critical Supersaturation Approximation. *International Journal of Heat and Mass Transfer*, 10:1267–1279, 1967.

- [35] W. E. Schiesser. The Numerical Method of Lines. Academic Press, Inc., San Diego, 1991.
- [36] K. Stephan and F. Mayinger. Technische Thermodynamik – Vol. 2: Mehrstoffsysteme und chemische Reaktionen. Springer Verlag, 1991.
- [37] J. G. van Leersum. Heat and Mass Transfer in Regenerators. PhD thesis, Department of Mechanical Engineering, Monash University, Australia, 1975.
- [38] J. G. van Leersum and P. J. Banks. Equilibrium Heat and Mass Transfer in Regenerators in which Condensation Occurs. International Journal for Heat and Mass Transfer, 20, 1977.
- [39] J. G. van Leersum and Ambrose C. W. Comparison between Experiments and a Theoretical Model of Heat and Mass Transfer in Rotary Regenerators with Nonsorbing Matrices. Journal of Heat Transfer, 103:189–195, May 1981.
- [40] R. Vauth. Wärme- und Stoffaustausch in Regenerativ-Wärmetauschern mit rotierenden nicht-adsorbierenden Speichermassen. Forschungsberichte des Deutschen Kälte- und Klimatechnischen Vereins, 1979.
- [41] VDI-Verlag. VDI-Wärmeatlas - Berechnungsblätter für den Wärmeübergang - 6th edition, 1991.
- [42] P. A. Zegeling, J. G. Verwer and J. C. H. van Eijkeren. Application of a Moving-Grid Method to a Class of 1D Brine Transport Problems in Porous Media, NM-R9112. Technical report, Centrum for Wiskunde en Informatica, CWI, Amsterdam, 1991.